J Appl Electrochem (2009) 39:1889–1895
DOI 10.1007/s10800-009-9896-0

ORIGINAL PAPER

Preparation of platinum nanoparticles on polyaniline-coat multi-walled carbon nanotubes for adsorptive stripping voltammetric determination of formaldehyde in aqueous solution

Guan-Ping Jin · Juan Li · Xia Peng

Received: 16 October 2008 / Accepted: 14 April 2009 / Published online: 2 May 2009

Abstract Platinum nanoparticles on polyaniline-coat multi-walled carbon nanotubes were fabricated by electrochemical method at paraffin-impregnated graphite electrode (Pt/PAN/MWCNTs). The material was characterized by various methods including field emission scanning electron microscope (FE-SEM), X-ray diffraction (XRD), X-ray photoelectron spectroscopy (XPS), and electrochemical techniques. The electrode has been effectively applied toward formaldehyde (HCHO) sensing. A good linear response curves from 1×10^{-9} to 1×10^{-3} M can be obtained with a lower detection limit of 4.6×10^{-11} M (S/N 3). The successful preparation of nanocomposites opens a new path to fabricate the promising sensor for HCHO.

Keywords Electrodeposition · Platinum nanoparticles · Polyaniline · Multi-walled carbon nanotubes · Formaldehyde sensing

1 Introduction

Formaldehyde (HCHO) is a very useful chemical material broadly applied in building plates, plywood, lacquer materials, and fuel cell [1]. However, it shows a bad influence on human's health such as central nervous, blood and immune systems, and could result in stunted growth, blindness, and respiratory diseases [2]. HCHO was found in more than 2,000 products to which many industrial workers were exposed on a daily basis. The permissible level of HCHO in industrial areas was set in 0.5–2.0 ppm [3]. All these facts convincingly demonstrate the requirement for accurate HCHO determination. Some attempts were reported to develop HCHO sensors due to its electrochemical activity with Pt, Ru, and Au electrocatalysts [4–8]. The electric polyaniline supporting nano-Pt and Pd were involved to develop HCHO fuel cell [4, 9–15]. Formaldehyde oxidation scheme was recently reported on Pt single crystals which involved adsorbed intermediates of CO_{ad}, H_2COO_{ad}, and HCOOH (Scheme 1) [16, 17]. However, nano-Pt/polyaniline showed a low sensitivity for sensing of HCHO, polyaniline film modified by nano-Pt displayed a poor stability, which limits the development of HCHO sensors and fuel cell [4, 15]. Therefore, the preparation of novel electrode materials with higher activity and good stability become potentially important.

As we know, the introduction of MWCNTs into a polymer matrix can improve electrical conductivity and mechanical properties for the original polymer matrix [18–20]. Meanwhile, MWCNTs have been regarded as a new support for metal catalysts due to its small size, high chemical/thermal/mechanical stabilities, and large surface area to volume ratio [21–23]. However, till today only one investigation has been studied that single-walled carbon nanotubes/polyaniline composite was used to support materials of Pt nanoparticles for HCHO fuel cell [11]. It is insufficient for HCHO sensing study.

In our opinion, the electrosynthesis of Pt/PAN/MWCNTs nanocomposite has not been achieved so far for HCHO sensing. In this work, we suggest a simple approach for electrosynthesis of platinum nanoparticles on

G.-P. Jin · J. Li · X. Peng
Anhui Key Laboratory of Controllable Chemistry Reaction & Material Chemical Engineering, Hefei 230009, People's Republic of China

G.-P. Jin (✉) · J. Li · X. Peng
Department of Application Chemistry of School of Chemical Engineering, Hefei University of Technology, Hefei 230009, People's Republic of China
e-mail: jgp@hfut.edu.cn

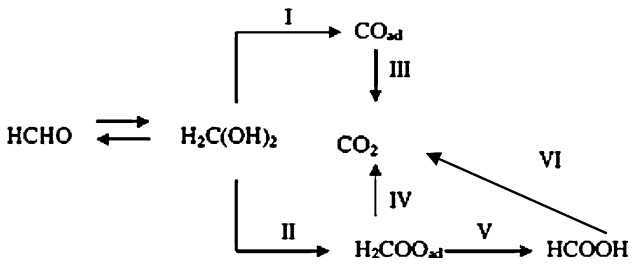

Scheme 1 The oxidation scheme of formaldehyde at Pt electrode

polyaniline-coat multi-walled carbon nanotubes film. The electroanalysis of HCHO has been investigated at the nanocomplex modified electrode in detail.

2 Experiment section

2.1 Reagents and equipment

Chemical reagents were obtained from Sun Nanotech. Co. Ltd., China as follows: MWCNTs with diameters of 10–30 nm and lengths of 1–10 μm were synthesized by catalytic decomposition of CH_4 on a NiMgO catalyst [21]. Aniline, formaldehyde, choline, and potassium tetrachloroplatinate (II) (K_2PtCl_4) were purchased from Chemical Reagent Company of Shanghai (China). All the reagents were used without further purification. All solutions and subsequent dilutions were prepared using purified water (prepared in a quartz apparatus). High purity nitrogen gas was used for deaeration.

Electrochemical measurements were performed with a model CHI 660 B electrochemical analyzer (Cheng-Hua, Shanghai, China). A paraffin-impregnated graphite electrode (WGE) with geometric area of 0.125 cm^{-2} was saved as working electrode [21]. A saturated calomel electrode (SCE, KCl) was used as the reference electrode and a platinum wire was used as the auxiliary electrode. The electrochemical experiments were performed in homemade gas cell detailed in literature [24]. Field emission scanning electron microscope (FE-SEM) images were obtained on a JSM-600 field emission scanning electron microanalyser (JEOL, Japan). XPS spectra were recorded by using an ESCALA-BMK_2 spectrometer (Vg corporation, UK) with a Mg-Alpha X-ray radiation as the source for excitation. X-ray diffraction (XRD) data of the samples were collected using a Rigaku D/MAX-rB diffractometer with Cu Kα radiation.

2.2 Preparation of platinum nanoparticles on polyaniline-coat multi-walled carbon nanotubes

The 10 mg MWCNTs were dispersed in 10 mL of mixed acid solution of nitric acid and perchlorate acid (7:3). The mixed solution was ultrasonically agitated for 7 h. The MWCNTs were washed with doubly distilled water to a neutral pH, then washed with acetone and dried in air. About 2.5 mg of mixed acid-treated MWCNTs were dispersed in 10 mL of acetone with the aid of ultrasonic agitation to give 0.25 mg mL^{-1} black suspension. The WGE electrode was step by step polished to a mirror-like finish with fine wet emery paper (grain size 1000, 3000, and 4000), followed by sonication in ethanol and water for 15 min, respectively. After cleaning, the choline modified WGE (Ch/WGE) with a positive charge was fabricated using the anode oxidation method by C–O bond to bond MWCNT with charge [21]. Then, 30 μL of the suspension was directly coated on Ch/WGE and evaporated in the solvent at room temperature (MWCNTs/Ch/WGE).

The polyaniline-coat MWCNTs was formed using cyclic voltammetry method (CV) in 0.01 M aniline/0.5 M H_2SO_4 (PAN/MWCNT/Ch/WGE). After rinsing with distilled water, the PAN/MWCNTs/Ch/WGE was transferred into a aqueous solution including 0.1 mM K_2PtCl_4/0.1 M H_2SO_4 at constant potential of −0.3 V with 400 s to form –NH–$PtCl_4^-$ complexes, then, the complexes were conversed to form platinum nanocomposites by successively potential cycling from −0.4 to 1.6 V with 25 cycles in 0.1 M H_2SO_4. The electrode was employed as the working electrode for HCHO electroanalysis (Pt/PAN/MWCNTs/Ch/WGE). WGE and MWCNTs/Ch/WGE were followed same process to form Pt/WGE and Pt/MWCNTs/Ch/WGE.

3 Results and discussion

3.1 Electrochemistry of Pt/PAN/MWCNTs/Ch/WGE

The electrochemical polyaniline can be observed at MWCNTs/Ch/WGE in Fig. 1a, inset. There is only one pair of peaks for the first cycle, on the subsequent cycling, three pair of peaks can be seen. The two sets of peaks locates at leucoemeraldine/emeraldine and emeraldine/pernigraniline transformations, respectively, and the third pair of peaks in the middle is attributed to the defects in the linear structure of the polymer [25].

In order to prepare the Pt/PAN/MWCNTs/Ch/WGE electrode, the PAN/MWCNTs/Ch/WGE was transferred into 0.1 mM K_2PtCl_4/0.1 M H_2SO_4 at constant potential of −0.3 V with 400 s, then, it was conversed by successively CV from −0.4 to 1.6 V in 0.1 M H_2SO_4. Figure 1 shows the CVs of bare WGE (a), MWCNTs/Ch/WGE (b), PAN/MWCNTs/Ch/WGE (c), Pt/MWCNTs/Ch/WGE (d), and Pt/PAN/MWCNTs/Ch/WGE (e) in 0.5 M H_2SO_4. It can be seen that one pair of peaks (0.53/0.21 V) at MWCNTs/Ch/WGE matching oxygenous functions. The three small pair of peaks at same position at PAN/MWCNTs/Ch/WGE

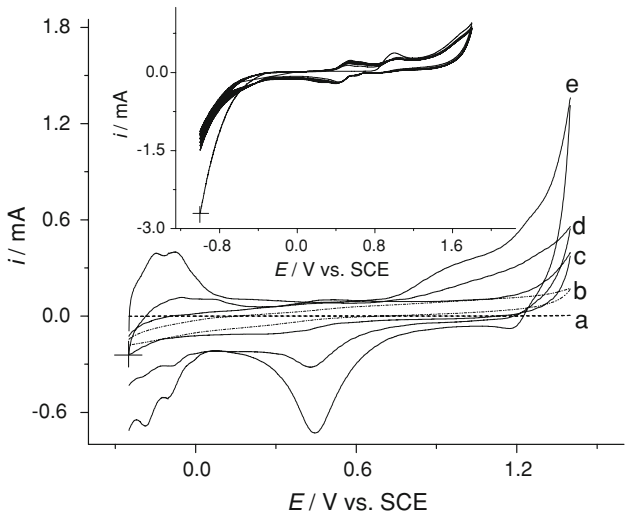

Fig. 1 CVs of bare WGE (a), MWCNTs/Ch/WGE (b), PAN/MWCNTs/Ch/WGE (c), Pt/MWCNTs/Ch/WGE (d), and Pt/PAN/MWCNTs/Ch/WGE (e) in blank H_2SO_4. Inset: CVs of MWCNTs/Ch/WGE in 0.01 M aniline. Buffer: 0.5 M H_2SO_4. Scan: 50 mVs^{-1}

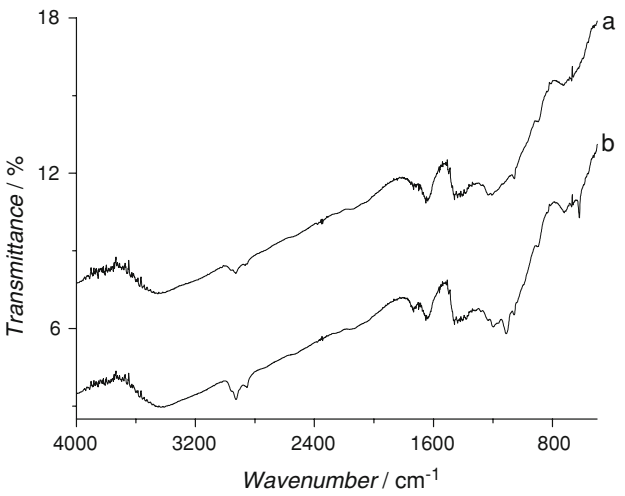

Fig. 2 IR of PAN coat—MWCNTs using CV with 30 (a) and 60 (b) scans in 0.01 M aniline

corresponding to polyaniline. The reversible hydrogen adsorption/desorption peaks (−0.20 and −0.1 V), preoxidation/reduction peaks (0.96/0.45 and 1.27/1.18 V) at Pt/MWCNTs/Ch/WGE and Pt/PAN/MWCNTs/Ch/WGE, the later response is higher than that of former, it suggests an advantageous adsorption of PAN/MWCNTs film toward $PtClO_4^-$.

3.2 Physical characterization and structural studies

Figure 2 shows the infrared spectra of polyaniline-coat MWCNT using CV with 30 (a) and 60 (b) scans. The FTIR characteristic bands of PAN are observed and in line with literatures [26, 27], which include C=N and C=C stretching vibrations for quinoid and benzenoid rings at 1,625 and 1,450 cm^{-1}, C–N stretching vibrations for benzenoid ring at about 1,310 and 1,250 cm^{-1}, the plane bending vibration of C–H at 1,100 cm^{-1}, and the out-of-plane bending vibration of C–H at 824 cm^{-1}. The peak at 1,735 suggests carboxylic acid groups presented on the surface of MWCNTs [16].

Figure 3a shows the FE-SEM micrograph of Pt/PAN/MWCNT/Ch/WGE before (inset) and after CV conversion. Some nanoparticles can be seen before the CV conversion, plentiful and uniformly dispersed nanoparticles can be readily seen after CV conversion and in line with the Scheme 2. As shown in Fig. 3b, the Pt nanoparticles can also be quickly electrodeposited on PAN/MWCNTs film with accumulative effect using CV method in $K_2PtCl_4/NiSO_4/H_2SO_4$.

Figure 4 shows the XRD of Pt/PAN/MWCNTs nanocomposites, all the peaks at different angles (2θ) are from Pt. A small shoulder at about 55° is matching to C (004). The diffraction peaks for Pt (39.8°, 46.2°, and 68°) are matching to fcc Pt (111), (200), and (220) [9, 11, 28]. The average grain size of the fcc Pt particles is calculated to be 10.6 nm by Scherrer equation. These document a successful deposition of Pt nanoparticles on PAN/MWCNTs film. It implies that the FE-SEM micrograph was formed by plentiful of nanoparticles (Fig. 3).

After the PAN/MWCNTs/Ch/WGE was transferred into 0.1 mM K_2PtCl_4/0.1 M H_2SO_4 at constant potential of −0.3 V with 400 s, the XPS of the complex film can be observed in Fig. 5 and the date were summarized in Table 1. $Pt_{4f7/2}$ and $Pt_{4f5/2}$ for Pt are shown at 71.5 and 74.8 eV with the theoretical ratio of 4:3 matching to the zero-valent metallic state, which is regnant in the quantity (64%). The peaks for Pt^{4+} can be seen at 72.6 and 75.9 eV corresponding to amino and $PtCl_4^-$ complex due to electrostatic adsorption (36%). It is noted that the two ion peaks cannot be seen after the complex film conversed in H_2SO_4 (no show). Therefore, Scheme 2 can be suggested in the following: polyaniline film was electrosysynthesized on MWCNTs to form electric film with amidocyanogen. The $PtCl_4^-$ was adsorbed at the polyaniline-coat MWCNTs at constant potential in K_2PtCl_4/H_2SO_4; meanwhile, 64% is reduced to form Pt nanoparticles at this potential, then the remainder is conversed to form the nanocomposites using CV in H_2SO_4.

3.3 The electrochemistry of formaldehyde at Pt/PAN/MWCNTs/Ch/WGE

Figure 6A shows the CVs of 0.3 mM HCHO at WGE (a), MWCNTs/Ch/WGE (b), PAN/MWCNTs/Ch/WGE (c), Pt/WGE (d), Pt/MWCNTs/Ch/WGE (e), and Pt/PAN/

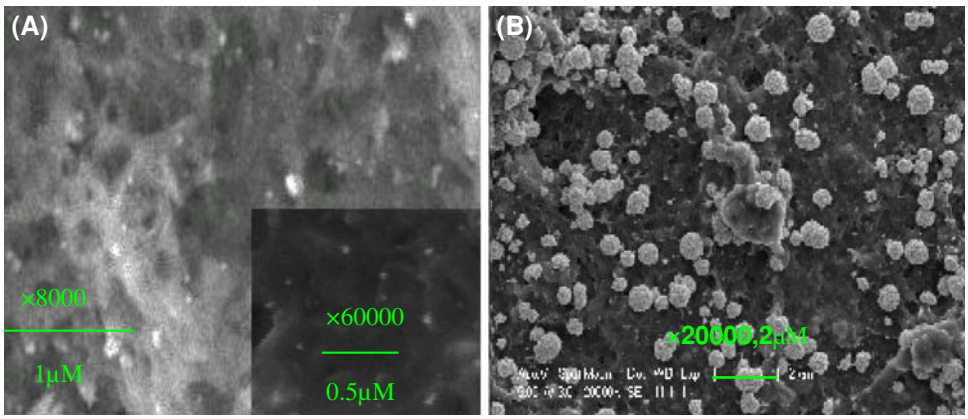

Fig. 3 **a** FE-SEM micrograph of Pt/PAN/MWCNTs/Ch/WGE before (inset) and after CV conversion. **b** FE-SEM micrograph of Pt/PAN/MWCNTs/Ch/WGE by direct electrodeposition in K_2PtCl_4/$NiSO_4$/H_2SO_4

Scheme 2 The electrochemical synthesis scheme of Pt/PAN/MWCNTs/Ch/WGE

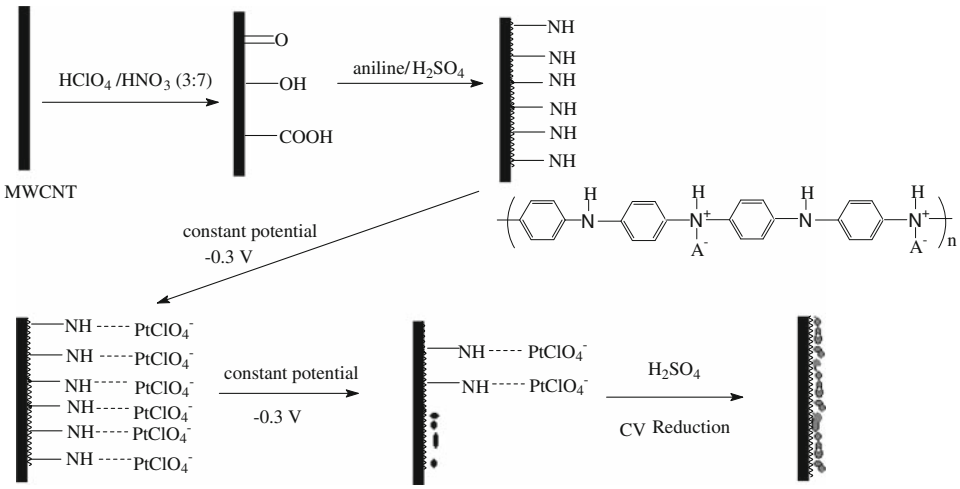

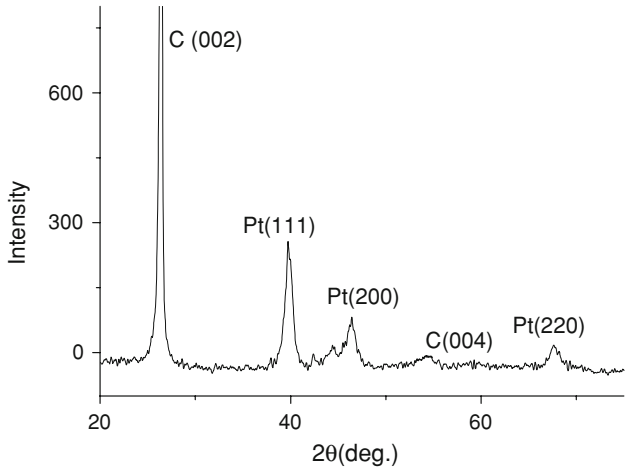

Fig. 4 XRD of Pt/PAN/MWCNTs

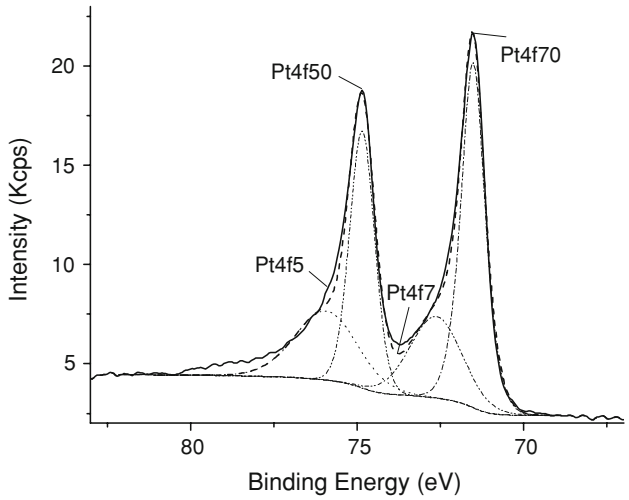

Fig. 5 XPS of Pt/PAN/MWCNTs before CV conversion

MWCNTs/Ch/WGE (f). The different increase on peak current can be observed at these modified electrodes compared with bare WGE, these suggest that MWCNTs, PAN, and nano-Pt show electrocatalysis toward the HCHO redox; among these, the effect at Pt/PAN/MWCNTs/Ch/WGE is the best. The inset shows the CVs of 0.0 (dash) and 0.3 mM HCHO (solid) at Pt/WGE (1) and Pt/PAN/MWCNTs/Ch/WGE (2). As can be seen in Fig. 6B, three peaks at 0.47, 0.67, and 1.27 V can be observed at Pt/WGE, in which HCHO was first oxidized to form CO_{ad} at low potential, H_2COO_{ad} at about 0.5 V, and CO_2 at high potential matching to Scheme 1 [9, 13]. However, only a significant increase can be seen at 1.27/1.18 V at Pt/PAN/

Table 1 XPS date of the Pt/PAN/MWCNT/Ch complex formed at −0.3 V with 400 s in $K_2PtCl_4/NiSO_4/H_2SO_4$

Name	Peak	At.%
N_{1s} A	400.33	2.63
N_{1s} B	401.94	1.11
Pt_{4f0}	71.52	11.66
Pt_{4f0}	74.85	8.62
Pt_{4f}	72.63	5.65
Pt_{4f}	75.93	5.79
Cl_{2p} A	198.24	0.24
Cl_{2p} A	199.84	0.11
Cl_{2p}·B	200.11	0.29
Cl_{2p}·B	201.71	2.99

MWCNTs/Ch/WGE (inset) with improved reversibility. The reason is probably relative to that CO_{ad} and H_2COOH formed by HCHO oxidation could be quickly conversed into CO_{2ad}, then, reduced to form H_2COOH at Pt/PAN/MWCNTs/Ch/WGE.

The effect of accumulation potential and time toward HCHO oxidation were, respectively, investigated at Pt/PAN/MWCNTs/Ch/WGE. Figure 6C shows that the oxidation peak's current is increasing with enhancing of the accumulation potential. It reaches the largest at 0.3 V, and evenness with an adsorption balance (potential > 0.4 V). As shown in the inset, the oxidation peak's current is increasing with delaying of the time. It reaches the largest at 10 min, then, it is getting a balance. Thus, the accumulation potential of 0.3 V and accumulation time of 10 min is optimum to obtain high sensitivity (Fig. 7).

In order to meet demand of quick detection, it is noticed that the oxidation peak's current is linear in a range of 1×10^{-9} to 1×10^{-3} even in accumulation time of 2.0 min under the accumulation potential of 0.3 V, the equation is of $i\ (A) = 1.3 \times 10^{-3} + 1.13 \times 10^{-4}$ C(M) ($R = 0.999$; LOD $= 2.1 \times 10^{-10}$ M, $3 \times \sigma$; SOD $=$ 1.13%, $n = 5$). Table 1 summaries the results of various method for HCHO sensing [4–8, 29–32]. In comparison with the reported results such as biosensors, semiconductor sensors, and odor sensor, the present work shows a better sensitivity (Table 2).

Interference was investigated for detection of HCHO. Some electrochemical gases such as H_2, CO, O_2, NO, and NO_2 interfere the detection. The interferences have to be eliminated before the detection of HCHO.

The stability of the electrode was also investigated. The Pt/PAN/MWCNTs/Ch/WGE showed high stability if stored in 0.5 M H_2SO_4 after use. Only 3% decrease in current response was observed for the first 2 days, 6% for

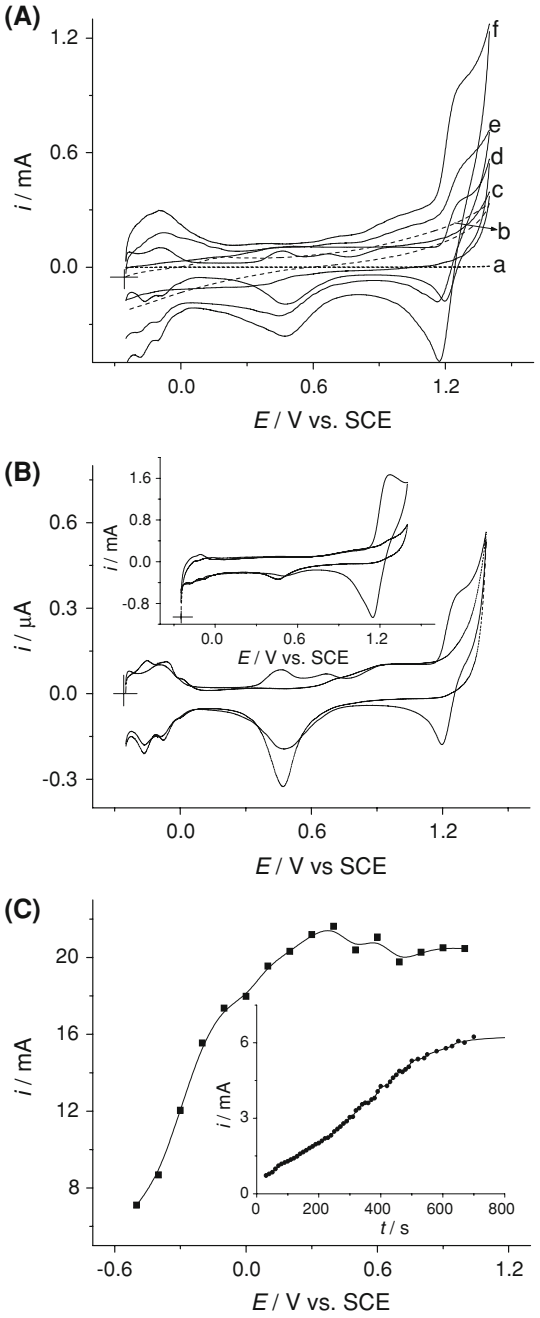

Fig. 6 **A** CVs of 0.3 mM HCHO (1.27 V) at WGE (a), MWCNTs/Ch/WGE (b), PAN/MWCNTs/Ch/WGE (c), Pt/WGE (d), Pt/MWCNTs/Ch/WGE (e), and Pt/PAN/MWCNTs/Ch/WGE (f). Accumulation potential: 0.3 V; Accumulation time: 2 min. **B** CVs of 0.0 (dash) and 0.3 mM HCHO (solid) at Pt/PAN/MWCNTs/Ch/WGE and Pt/WGE (inset). Accumulation potential: 0.3 V; Accumulation time: 2 min. **C** Oxidation currents of 0.1 mM HCHO (1.27 V) depend on adsorption potential at Pt/PAN/MWCNTs/Ch/WGE in accumulation time of 2 min. Inset: the oxidation peak currents of 0.1 mM HCHO (1.27 V) depend on time at adsorption potential of 0.3 V at Pt/PAN/MWCNTs/WGE. Buffer: 0.5 M H_2SO_4. Scan: 50 mVs^{-1}

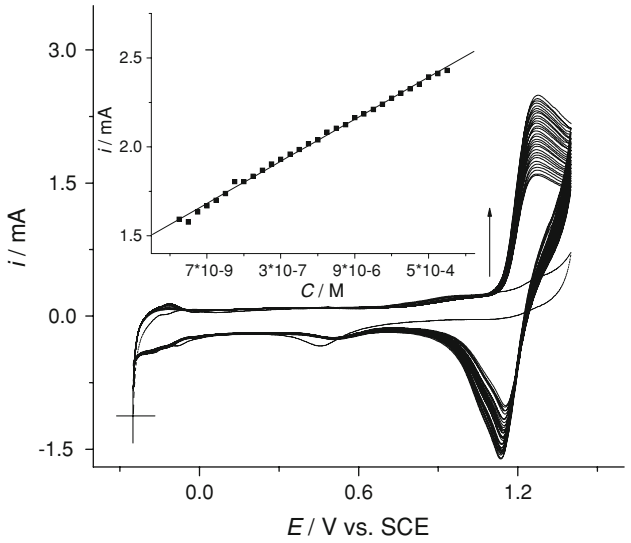

Fig. 7 CVs of HCHO ($1 \times 10^{-9} \rightarrow 1 \times 10^{-3}$ M, every 2×10^{-9}, 2×10^{-8}, 2×10^{-7}, 2×10^{-6}, 2×10^{-5}, and 2×10^{-4} M) at Pt/PAN/MWCNTs/Ch/WGE. Inset: the oxidation peak currents of HCHO depend on the concentration. Accumulation potential: 0.3 V; Accumulation time: 2 min. Buffer: 0.5 M H_2SO_4. Scan: 50 mVs^{-1}

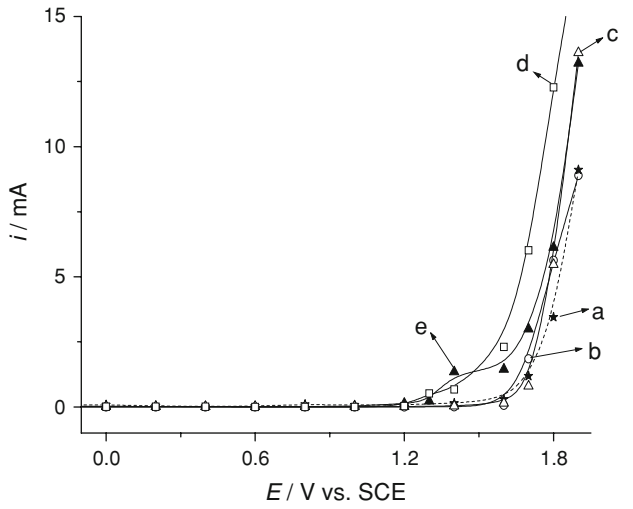

Fig. 8 The steady-state polarization curves of 0.1 mM HCHO at WGE (a), MWCNTs/Ch/WGE (b), PAN/MWCNTs/Ch/WGE (c), Pt/WGE (d), and Pt/PAN/MWCNTs/Ch/WGE (e). Accumulation potential: 0.3 V; Accumulation time: 2 min. Buffer: 0.5 M H_2SO_4. Scan: 50 mVs^{-1}

5 days, and 13% for a month. Comparatively, the Pt/WGE and Pt/PAN/WGE showed lower stability for storage in 0.5 M H_2SO_4, both 17% and 26% decrease was found for the first 1 day. The reason will be further studied.

Figure 8 shows that the steady-state polarization curves of 0.3 mM HCHOat WGE (a), MWCNT/Ch/WGE (b), PAN/MWCNT/Ch/WGE (c), Pt/WGE (d), and Pt/PAN/MWCNT/Ch/WGE (e). It can be seen that all the electrodes display small electrocatalysis for HCHO oxidation as the polarization potential <1.2 V. However, an excellent effect can be observed at the Pt/PAN/MWCNT/Ch/WGE as the polarization potential >1.27 V with a good stability in a range from 1.27 to 1.57 V compared with Pt/WGE. Meanwhile, an obviously improved effect can be observed at PAN/MWCNT/Ch/WGE and MWCNT/Ch/WGE as the polarization potential >1.6.

4 Conclusion

This work suggests a new route for electrosynthesis of platinum nanoparticles on polyaniline-coat multi-walled carbon nanotubes. The nanocomposites were successfully used as electroanalysis of HCHO with a high sensitivity and good stability. Further studies shall be expended to the practical detection of HCHO and fuel cells application.

Table 2 Various sensors for formaldehyde detection

Type	Arrangement	Detection limit (ppm)	Reference
Amperometric	Formaldehyde dehydrogenase	30	[3]
Amperometric	Au/Nafion/0.1 M H_2SO_4	0.013	[4]
Amperometric	Formaldehyde dehydrogenase and a Os(bpy)2-poly(vinylpyridine) (POs-EA)/screen-printed electrode	30	[5]
Amperometric	Formaldehyde dehydrogenase	0.03	[6]
Amperometric	Formaldehyde dehydrogenase/Pt polytetrafluoroethylene	0.41	[7]
Amperometric	Formaldehyde dehydrogenase/exogenous cofactor/Si/SiO_2/Si_3N_4	300	[8]
Semiconductor	CdO-mixed In_2O_3	10	[29]
Semiconductor	Cataluminescence-based gas sensor	0.06	[30]
UV	Porous glass impregnated with Schiff's reagent	0.01	[31]
Odor	A quartz crystal microbalance	615	[32]
This work	Accumulation time: 2 min	0.046	

Acknowledgements The authors gratefully acknowledge financial support from Natural Science Foundation of Anhui Province of China (No. 070415210), Science and Technology Program Foundation of Hefei City (No. 20071032), and Doctor Foundation of Hefei University of Technology (2005).

References

1. Gerberich HR, Seaman GC (1994) Encyclopedia of chemical technology, vol 11, 4th edn. Wiley, New York, USA, p 929
2. Flyvholm MA, Andersen P (1993) Am J Ind Med 24:533
3. Demkiv O, Smutok O, Paryzhak S, Gayda G, Sultanov Y, Guschin D, Shkil H, Schuhmann W, Gonchar M (2008) Talanta 76:837
4. Knake R, Jacquinot P, Hauser PC (2001) Electroanalysis 13:631
5. Herschkovitz Y, Eshkenazi I, Campbell CE, Rishpon J (2000) J Electroan Chem 491:182
6. Achmann S, Hämmerle M, Moos R (2008) Electroanalysis 20:410
7. Mitsubayashi K, Nishio G, Sawai M, Saito T, Kudo H, Saito H, Otsuka K, Noguer T, Marty JL (2008) Sens Act B 130:32
8. BenAli M, Gonchar M, Gaydac G, Paryzhak S, Maaref MA, Jaffrezic-Renault N, Korpan Y (2007) Biosens Bioelectron 22:2790
9. Mascaro LH, Goncalves D, Bulhões LOS (2004) Thin Solid Films 461:243
10. Santos MC, Bulhões LOS (2004) Electrochim Acta 49:1893
11. Wang Z, Zhu ZZ, Shi J, Li HL (2007) Appl Surf Sci 253:8811
12. Wu YM, Li WS, Lu J, Du JH, Lu DS, Fu JM (2005) J Power Sources 145:286
13. Ma CA, Li MC, Zheng YF, Liu BY (2005) Electrochem Solid-State Lett 8:G122
14. Villullas HM, Mattos-Costa FI, Nascente PAP, Bulhões LOS (2004) Electrochim. Acta 49:3909
15. Park S, Xie Y, Weaver MJ (2002) Langmuir 18:5792
16. de Lima RB, Massafera MP, Batista EA, Iwasita T (2007) J Electroan Chem 603:142
17. Batista EA, Iwasita T (2006) Langmuir 22:7912
18. Schadler LS, Giannaris SC, Ajayan PM (1998) Appl Phys Lett 73:3842
19. Wagner HD, Lourie O, Feldman Y, Tenne R (1998) Appl Phys Lett 72:188
20. Qian D, Dickey EC, Andrews R, Rantell T (2000) Appl Phys Lett 76:2868
21. Jin GP, Ding YF, Zheng PP (2007) J Power Sources 166:80
22. Tian ZQ, Jiang SP, Liang YM, Shen PK (2006) J Phys Chem B 110:5343
23. Villers D, Sun SH, Serventi AM, Dodelet JP, Desilets S (2006) J Phys Chem B 110:25916
24. Barrosse-Antle LE, Silvester DS, Aldous L, Hardacre C, Compton RG (2008) J Phys Chem C 112:3398
25. Zhang L, Lian JY (2007) J Electroan Chem 611:51
26. Cheng D, Ng SC, Chan HSO (2005) Thin Solid Films 477:19
27. Zeng XR, Ko TM (1997) Polym J Sci Part B 35:1993
28. Wu G, Li L, Li JH, Xu BQ (2005) Carbon 43:2579
29. Chen T, Q.Liu J, Zhou ZL, Wang YD (2008) Sens Act B 131:301
30. Zhoua K, Ji X, Zhang N, Zhang X (2006) Sens Act B 119:392
31. Maruo YY, Nakamuraa J, Uchiyamab M, Higuchi M, Izumi K (2008) Sens Act B 129:544
32. Feng L, Liu Y, Zhou X, Hu J (2005) J Colloid Interface Sci 284:378